
**Liquid Crystals**
Publication details, including instructions for authors and subscription information:
http://www.informaworld.com/smpp/title~content=t713926090

# Computer modelling and simulation of thermotropic and lyotropic alkyl glycoside bilayers

Teoh Teow Chong[a]; Thorsten Heidelberg[a]; Rauzah Hashim[a]; Saadullah Gary[a]
[a] Department of Chemistry, Faculty of Science, University of Malaya, 50603 Kuala Lumpur, Malaysia

**To cite this Article** Chong, Teoh Teow , Heidelberg, Thorsten , Hashim, Rauzah and Gary, Saadullah(2007) 'Computer modelling and simulation of thermotropic and lyotropic alkyl glycoside bilayers', Liquid Crystals, 34: 2, 267 — 281
**To link to this Article: DOI:** 10.1080/02678290601130192
**URL:** http://dx.doi.org/10.1080/02678290601130192

*Liquid Crystals*, Vol. 34, No. 2, February 2007, 267–281



# Computer modelling and simulation of thermotropic and lyotropic alkyl glycoside bilayers

TEOH TEOW CHONG, THORSTEN HEIDELBERG, RAUZAH HASHIM* and SAADULLAH GARY**
Department of Chemistry, Faculty of Science, University of Malaya, 50603 Kuala Lumpur, Malaysia

(*Received 1 March 2006; accepted 18 September 2006*)

Simulations on bilayers have previously proven their ability to provide insights to membrane function, e.g. cell fusion. Most simulations are based on the major components of cell membranes, which are phospholipids and cholesterol. Membranes can be explained based on hydrophilic and hydrophobic interactions permeated through hydrogen bonding, van der Waals interactions and repulsion forces. Whereas especially phospholipids have gained significant attention in bio-related modelling and simulations, glycolipids, which constitute another major component of cell membranes, have not been likewise studied. Here we present the simulation of bilayers for the six most common and simple stereoisomeric glycolipids, namely the α- and β-octyl glycosides of glucose, galactose and mannose, in both thermotropic and lyotropic systems. All these compounds form thermotropic smectic A phases and can exhibit lyotropic lamellar assemblies. We have studied the hydrogen bonding and linked the results to the temperature stability of the corresponding liquid crystal phase. Besides a mesophase-stabilizing effect of hydrogen bonding in general, we found that thermal stability appears to be particularly affected by intralayer hydrogen bonding. The simulations also confirmed a significant difference in the density of the lipophilic region for α- and β-glycosides, which has previously been used to explain differences in clearing temperatures.



## 1. Introduction

Alkyl glycosides are simple glycolipids that have proven useful tools in biology and chemistry, due to their ability to act as non-ionic surfactants. For example, commercially available alkyl glucosides [1] have been applied to stabilize, reconstitute, purify and crystallize membrane proteins and membrane-associated protein complexes without denaturation. Besides their simple surfactant applications [2], especially as emulsifiers, alkyl glycosides also can form liposome-like vesicles, thus providing a potential target for drug carriers [3, 4]. In this study the three most simple and common alkyl glycosides, i.e. octyl glucopyranoside ($C_8$Glc), octyl galactopyranoside ($C_8$Gal) and octyl mannopyranoside ($C_8$Man), are investigated in both α- and β-anomeric form. These compounds only differ in the stereochemical orientation (axial or equatorial) of the hydroxyl groups at C2 and C4 and the alkoxy substituent at C1 of the sugar unit (figure 1). All of them, as far as they have been analysed (β-$C_8$Man and α-$C_8$Gal remain uninvestigated), show thermotropic smectic and lyotropic lamellar phases at low to moderate water concentrations [5]. Despite their structural similarity, the glycosides significantly vary in the transition temperatures. β-$C_8$Gal, for example, exhibit a smectic A phase at higher temperature (96–127°C) than β-$C_8$Glc (69–107°C) [5].

In an attempt to understand the variable clearing temperatures for stereoisomeric alkyl glycosides, we have applied computer simulations on bilayer structures for the six glycosides mentioned above. Glycolipid bilayer structures are based on a microphase separation of two incompatible molecular regions, i.e. the hydrophilic sugar part and the hydrophobic alkyl chain [6]. With respect to the number of hydroxyl groups in the investigated molecules and owing to their significantly higher bonding energy contribution compared to other intermolecular interactions, hydrogen bonds are believed to dominate the self-assembly of glycolipids, thus forming the major driving force for liquid crystal phases. We therefore analysed the hydrogen bonding patterns in the pure state and in the presence of water (lyotropic system) and tried to correlate our simulation results with published experimental clearing points. There have been several previous simulations on bilayers, performed by researchers such as van Buuren and Berendsen [7], Feller *et al.* [8] and Bogusz *et al.* [9]. Particularly interesting is the simulation of a membrane fusion by Ohta-lino *et al.* [10]. However, no evaluation

*Corresponding author.
**Permanent address: Chemistry Department, King Abdul Aziz University, Jeddah 21589, Saudi Arabia.

*Liquid Crystals*
ISSN 0267-8292 print/ISSN 1366-5855 online © 2007 Taylor & Francis
http://www.tandf.co.uk/journals
DOI: 10.1080/02678290601130192

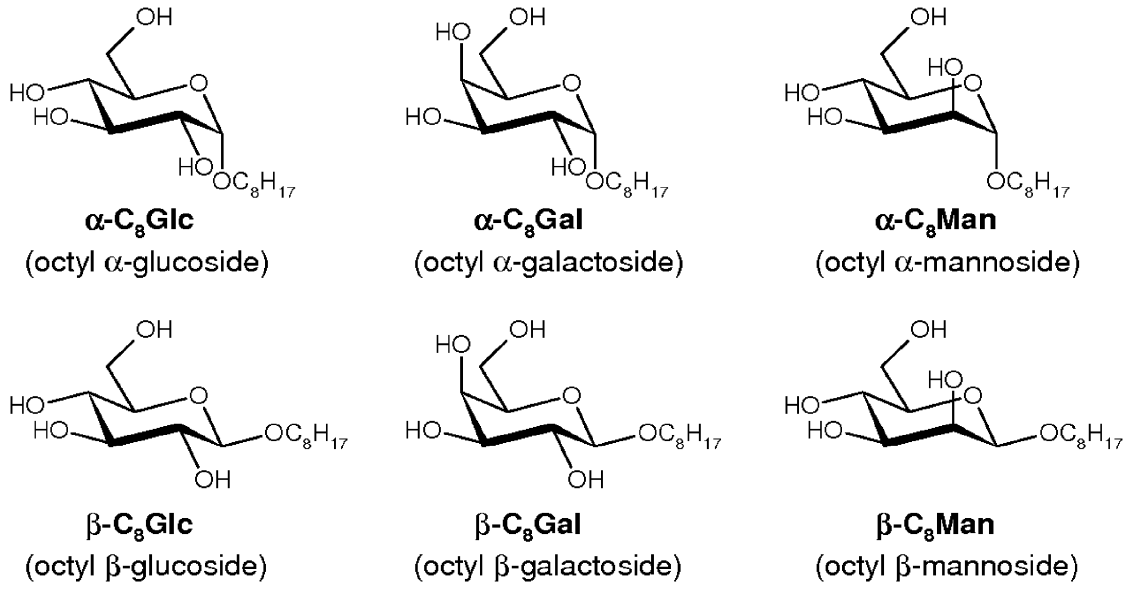


Figure 1. Chemical structures of the investigated glycosides.



of hydrogen bonding, such as the one in this study, has been carried out so far, due to the extensive requirements of computational resources for the simulation. In addition to the hydrogen bonding analysis, we also evaluated the bilayer spacings and the local density profiles (LDP). The density of the lipophilic region has been associated with the stability of glycolipids liquid crystals [5]. In order to evaluate this statement, we determined this density and correlated it to experimental clearing temperatures.

## 2. Methods

For each simulation 400 glycolipid molecules were arranged in two bilayers. Firstly, a monolayer comprising $10 \times 10$ parallel oriented glycolipids was built based on a cubic lattice pattern using the Hyperchem crystal builder. In accordance with recent findings [11], the alkyl tails of the glycosides are tilted towards the bilayer axis. Two monolayers were combined, alky tail to alkyl tail, to form the initial bilayer. This configuration was minimized in Hyperchem, to avoid breaking of the aggregation during the final simulation, and subsequently converted into PDB-format using Babel. The final minimization and the molecular dynamic runs were performed on Amber 7 [12] for a set of two of the above bilayers. In case of lyotropic systems, 550 water molecules were arranged on the top and at the bottom of each of the bilayers. This corresponds to a glycolipid concentration of about 85%. The temperature was set at 300 K and all simulations were carried out under constant pressure (NpT) in a cuboid periodic box. An equilibration time of 600 ps was applied with gradual decrease of group harmonic constraint force down from 500 to 0 kcal $mol^{-1}$ $Å^{-1}$, followed by a production time of 5 ns in 1 fs steps. Various computer facilities were used, but typically those were provided by UM CAD-CAM Geranium CRAY cluster comprising 16 nodes in the Engineering Faculty of University of Malaya. A 1 ns simulation took about 24 hours to complete.

Hydrogen bonding analyses were performed for every picosecond. Qualified OH–O hydrogen bonding were selected based on an O–O distance of 4 Å and an angle cut-off of 60°. This criterion is based on the Amber7 manual [12] recommendation of 3.5 Å (we increased the value to 4.0 Å) and 120° in ptraj, corresponding to 4.0 Å and 60° in carnal (figure 2).

Hydrogen bonding was classified into three types for the thermotropic and one additional type for lyotropic systems. The first separation differentiated between intermolecular (figure 3a) and intramolecular (figure 3b) hydrogen bonding. The former were further split into intralayer and interlayer interactions (figure 3c) [13]. This differentiation reflects the anisotropy of the layer-structure and correlates with expected energy differences for the cohesion of molecules within the same layer with respect to those belonging to different layers. Finally for lyotropic systems there remain interactions of sugar and water or solvent-solute hydrogen bonding (figure 3d).

Bilayer spacing was measured as the distance of the centres of mass for the first and the second bilayer, as shown in figure 4a. The values analysed this way are the averages based on all 5000 frames, recorded over the 5 ns simulation period. Alternatively the bilayer spacing was determined from a one-dimensional local density

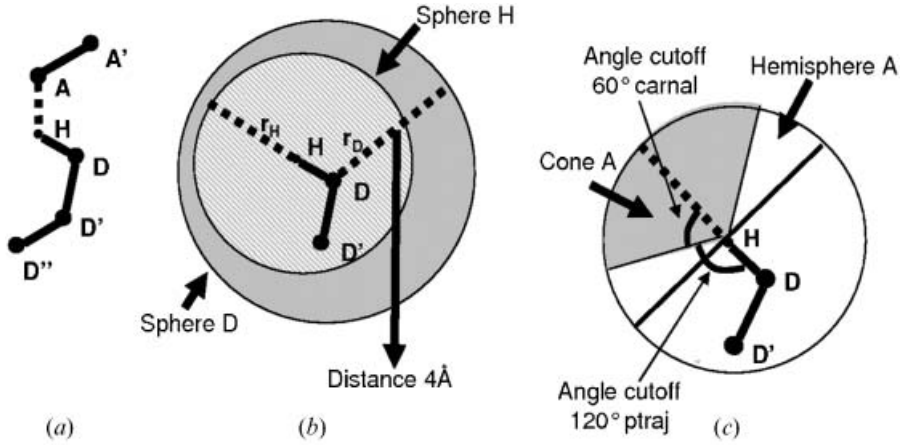


Figure 2. Hydrogen bonding selection criteria. (a) Spatial model of a hydrogen-bonding interaction (A=hydrogen acceptor, electron pair donor, D-H=hydrogen donor); (b) hydrogen-bonding selection spheres; (c) angle restriction for hydrogen bonding.

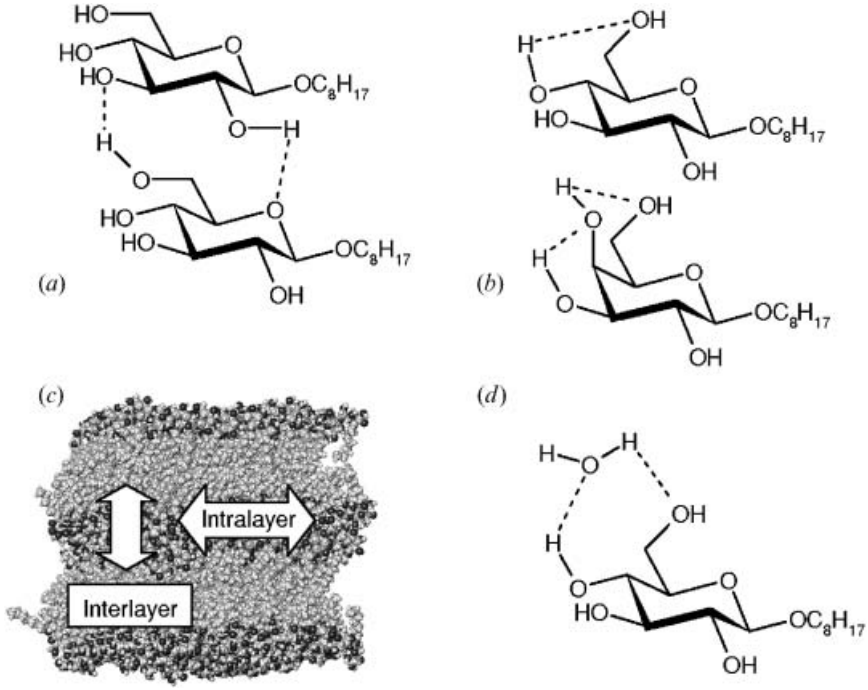


Figure 3. Classification of hydrogen bonding (dotted lines). (a) Intermolecular hydrogen bonding; (b) intramolecular hydrogen bonding; (c) illustration of inter- and intralayer hydrogen bonding (black=oxygen, grey=carbon, white=hydrogen); (d) solvent–lipid hydrogen bonding.

profile (LDP, figure 4b). The latter approach avoids possible (minor) errors based on X- and Y-participation to the normally exclusively Z-based bilayer distance. This can happen if the centre of mass in bilayer plane differs slightly for the two bilayers. However, the LDP-based analysis could only be applied on single simulation frames and, therefore, is more limited with respect to precision. To avoid a systematic error due to a possible expansion or contraction of the bilayers over the simulation time, we evaluated the LDP for one frame each from the start and at the end of the simulation and applied the average. The error estimation considers statistical deviations as well as a limited accuracy of the applied method. The latter we estimated to $\pm 1$Å, based on 0.5–1Å intervals applied on simulation derived coordinates to determine the local density profiles.

The density of the lipid tail was estimated by the mass over volume in $g\,cm^{-3}$. The volume of the lipid tail was estimated by the HyperChem™ v6.0 Quantitative

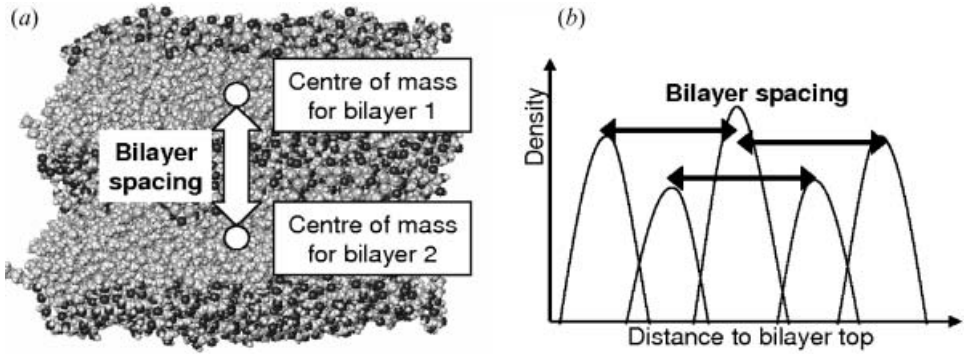


Figure 4. Determination of bilayer spacing. (a) Centre of mass approach; (b) local density profile approach.

Structure Activity Relationships Properties (QSAR Properties) [14] module. Internal surface areas between the hydrophilic and the hydrophobic regions of glycosides were estimated based on the dimensions of the periodic box along the bilayer. Box dimensions were determined for each nanosecond and averaged over the 5 ns simulation period.

### 2.1. *Estimation of clearing temperatures, $T_c$, from hydrogen bonding*

The clearing temperature was estimated using the relationship between energy and temperature derived from the Boltzmann equation. We assume that the main energy stabilizing the bilayer is based on hydrogen bonding and that all the hydrogen bonding are statistically equivalent in energy. Thus, to a good approximation the energy differences in the equations below may be replaced by the hydrogen bonding values.

Assuming that the difference in internal energy between the smectic (or the lamellar lyotropic) and the isotropic phase is the same for two stereoisomeric glycosides, e.g. $\beta$-$C_8$Glc and $\beta$-$C_8$Gal, we obtain the following equations based on the Boltzmann equation for internal energy, $E=k_BT$ where $k_B$=Boltzmann constant and $T$=temperature in Kelvin:

$$\frac{\Delta E_{\beta C_8\mathrm{Gal}}}{\Delta E_{\beta C_8\mathrm{Glc}}}=\frac{k_BT_{\beta C_8\mathrm{Gal}}}{k_BT_{\beta C_8\mathrm{Glc}}},$$
$$T_{\beta C_8\mathrm{Gal}}=\frac{\Delta E\beta C_8\mathrm{Gal}}{\Delta E\beta C_8\mathrm{Glc}}T_{\beta C_8\mathrm{Glc}}. \quad (1)$$

The clearing point for $\beta$-$C_8$Gal, $T_{\beta C_8\mathrm{Gal}}$, can, therefore, be estimated based on the reference clearing point for $\beta$-$C_8$Glc, $T_{\beta C_8\mathrm{Glc}}$. With respect to neglected energy contributions of factors other than hydrogen bonding, equation (1) should be limited to closely related structures only. Thus, we used separate correlations for $\alpha$- and $\beta$-glycosides.

Based on the uncertainties of the hydrogen bonding we can also estimate the error for the predicted clearing temperature $T_c$ as

$$\sigma T_{\beta C_8\mathrm{Gal}}=\sqrt{\left(\frac{T_{\beta C_8\mathrm{Glc}}}{\Delta E_{\beta C_8\mathrm{Glc}}}\sigma\left(\Delta E_{\beta C_8\mathrm{Gal}}\right)\right)^2+\left(\frac{T_{\beta C_8\mathrm{Glc}}\left(\Delta E_{\beta C_8\mathrm{Gal}}\right)}{\left(\Delta E_{\beta C_8\mathrm{Glc}}\right)^2}\sigma\left(\Delta E_{\beta C_8\mathrm{Glc}}\right)\right)^2}$$

where $\sigma T_{\beta C_8\mathrm{Gal}}$ is the standard deviation for the clearing temperature for $\beta$-$C_8$Gal based on $\beta$-$C_8$Glc.

## 3. Results

### 3.1. *Hydrogen bonding and clearing temperature, $T_c$, in thermotropic systems*

Our simulations reveal a significantly higher number of total inter-glycoside hydrogen bonding for $\alpha$-glycosides than for the $\beta$-analogues. Whereas the values per molecule indicate a small but noticeable effect of the sugar's configuration for $\alpha$-glycosides (table 1), $\beta$-$C_8$Glc and $\beta$-$C_8$Gal show identical results (both $3.5\pm0.1$). However, the intralayer hydrogen bonding for the galactoside ($2.9\pm0.1$) is significantly higher than for the glucoside ($2.7\pm0.1$). Since the intralayer hydrogen bonding is remarkably higher than the interlayer hydrogen bonding, we suggest that the higher clearing point for $\beta$-$C_8$Gal must be due to the higher intralayer hydrogen bonding. Thus, the correlation of clearing temperatures based on equation (1) applies these values instead of the total hydrogen bonding for $\beta$-glycosides.

Since intramolecular hydrogen bonding cannot be related to molecular cohesion, we did not primarily focus on them. However, the extent of intramolecular hydrogen bonding can affect intermolecular hydrogen bonding due to the competition of both for hydrogen atoms. Thus, intramolecular hydrogen bonding may indirectly be correlated to bilayer stability as well. In order to evaluate this possibility, we compared the values for the $\beta$-glycoside series. The data, displayed in table 2, indicate no effect for sugar epimers. Assuming

Table 1. Intermolecular hydrogen bonding analysis for thermotropic bilayers. $T_c$ calculation based on equation (1).

| | | α-Man | α-Gal | α-Glc | β-Gal | β-Glc | β-Man |
|---|---|---|---|---|---|---|---|
| H bonding | total | 3.96 ± 0.03 | 3.85 ± 0.04 | 3.8 ± 0.1 | 3.5 ± 0.1 | 3.5 ± 0.1 | 3.14 ± 0.04 |
| | intra-layer | 2.61 ± 0.02 (=66%) | 2.43 ± 0.04 (=63%) | 2.77 ± 0.03 (=73%) | 2.9 ± 0.1 (=82%) | 2.7 ± 0.1 (=77%) | 3.08 ± 0.03 (=98%) |
| | inter-layer | 1.35 ± 0.01 (=34%) | 1.42 ± 0.003 (=37%) | 1.0 ± 0.1 (=27%) | 0.64 ± 0.02 (=18%) | 0.81 ± 0.03 (=23%) | 0.61 ± 0.01 (=2%) |
| $T_c$ [°C] | exp. | 132 [5] 134 [15] | – | 116 [5] 118 [15] | 127 [5] 133 [15] | 107 [5] 108 [15] | – |
| | calc.[1, 3] | 132 ± 12 | 121 ± 12 | reference | – | – | – |
| | calc.[2, 4] | – | – | – | 107 ± 15 | reference | 68 ± 5 |
| | calc.[2, 3] | – | – | – | 135 ± 21 | reference | 160 ± 17 |

[1] ref. α-$C_8$Glc 116°C; [2] ref. β-$C_8$Glc 107°C; [3] total H bonding; [4] intralayer H bonding.

Table 2. Intramolecular hydrogen bonding.

| β-Gal | β-Man | β-Glc |
|---|---|---|
| 1.5 ± 0.5 | 1.5 ± 0.4 | 1.5 ± 0.4 |

this trend to be valid for the α-series as well, we concluded, that intramolecular hydrogen bonding may be ignored for this investigation.

Taking α-$C_8$Glc as reference ($T_c$=116°C), the calculated clearing temperature of α-$C_8$Man exactly matched the literature reported value of 132°C. The predicted value for α-$C_8$Gal of 121°C lies between the gluco- and the mannoside. For β-$C_8$Gal, we estimated $T_c$ as 135°C (based on 107°C for β-$C_8$Glc), which again is in good agreement with experimental values ranging from 127°C [5] to 133°C [15]. The prediction for β-$C_8$Man depends on the choice of either total inter-glycoside hydrogen bonding or just intralayer hydrogen bonding (table 1) and will be discussed later.

### 3.2. *Hydrogen bonding in lyotropic systems*

In lyotropic systems all inter-glycoside hydrogen bonding are decreased with respect to the thermotropic analogues. However, the impact of water on interlayer hydrogen bonding is, expectedly, significantly higher than for intralayer interaction. Whereas the latter only suffered a moderate decrease up to 30%, the former are almost reduced to zero in case of β-glycosides. For α-glycosides, however, interlayer (inter-glycoside) hydrogen bonding still remains a considerable cohesion factor. The descending order for total hydrogen bonding in lyotropic system differs from the thermotropic one only in the position of the α-glucoside (tables 1 and 3). An explanation for this behaviour is given in the discussion section.

Clearing temperatures for lyotropic systems are much less easy to compare than for thermotropic analogues, since the data depend on the concentration. Unfortunately, neither the experimental data for different glycosides, nor our simulations reflect the same concentration. Due to this systematic error, the potential accuracy of predictions is low and, a qualitative analysis appears more appropriate. As shown in table 3, the sequence of clearing points follows the one of the total hydrogen bonding. A slightly more extensive analysis follows in the discussion part.

### 3.3. *Local density profile (LDP) and bilayer spacing*

The local density profiles for all simulations are displayed in figures 5 and 6. We only observed minor differences for frames at the beginning and at the end of the simulation, therefore only one profile for each

Table 3. Intermolecular hydrogen bonding analysis for lyotropic bilayers. $T_c$ calculation based on equation (1).

| | | | α-Glc | α-Man | α-Gal | β-Gal | β-Glc | β-Man |
|---|---|---|---|---|---|---|---|---|
| H-bonding | inter-lipid | total | 2.5 ± 0.1 | 2.3 ± 0.1 | 2.3 ± 0.1 | 2.7 ± 0.1 | 2.5 ± 0.1 | 2.9 ± 0.1 |
| | | intra-layer | 2.23 ± 0.03 | 2.0 ± 0.1 | 2.03 ± 0.03 | 2.6 ± 0.1 | 2.4 ± 0.1 | 2.88 ± 0.03 |
| | | $\Delta_{aq\text{-}pure}$ | −8% | −18% | −28% | −10% | −11% | −6% |
| | | inter-layer | 0.24 ± 0.03 | 0.31 ± 0.04 | 0.30 ± 0.04 | 0.06 ± 0.02 | 0.06 ± 0.03 | 0 |
| | | $\Delta_{aq\text{-}pure}$ | −82% | −78% | −70% | −90% | −93% | −100% |
| | solvent–solute | total | 3.7 ± 0.3 | 3.7 ± 0.2 | 3.6 ± 0.1 | 3.0 ± 0.1 | 3.1 ± 0.2 | 2.5 ± 0.1 |
| | | water H-donor | 2.4 ± 0.1 | 2.7 ± 0.1 | 2.7 ± 0.1 | 2.3 ± 0.03 | 2.3 ± 0.1 | 1.9 ± 0.1 |
| | | water accept. | 1.3 ± 0.2 | 1.0 ± 0.1 | 0.90 ± 0.03 | 0.7 ± 0.1 | 0.8 ± 0.1 | 0.58 ± 0.02 |
| | | total | 6.2 ± 0.4 | 6.0 ± 0.3 | 5.9 ± 0.2 | 5.7 ± 0.4 | 5.6 ± 0.3 | 5.4 ± 0.2 |
| $T_c$ [°C] | | exp. | – | 140 [5] (6% aq) | – | 136 [5] (13% aq) | 122 [5] (19% aq) | – |
| | | calc. | 164 ± 37 | 150 ± 31 | 143 ± 26 | 129 ± 36 | reference | 108 ± 25 |

simulation is given. All LDPs show the expected microphase separation, exhibiting antipodal maxima and minima for the hydrophilic and the hydrophobic regions of the glycolipids. In lyotropic systems the density profile of water basically follows the one of the hydrophilic head group. However, for β-glycosides we notice the exhibition of a water-enriched domain that clearly separates two polar glycolipid regions. α-Glycosides on the other hand almost do not show this kind of behaviour.

Values for experimental and simulated bilayer spacing are summarized in table 4. β-Glycosides show significantly larger bilayer spacing than α-anomers. This applies both for thermotropic systems as well as for lyotropic analogues, where the bilayer spacing is increased to about 20% for β-glycosides to 25–30% for α-anomers. Whereas the simulations are in good agreement with SAXS determined data [5] for thermotropic systems of α-glycosides, the corresponding values for β-compounds exceed experimental data by nearly 10%. Lyotropic simulations overshoot experimental data to about 15%. The two methods for used for the determination of the bilayer spacing show no variations for β-glycosides, but differ slightly for the α-anomers, where LDP indicates higher values than the centres of mass approach. Interestingly the LDP-derived bilayer spacing proved more accurate for thermotropic systems, while the centres of mass based method was better for lyotropic systems.

### 3.4. *Internal microphase surface area and density of the hydrophobic tail region*

Internal microphase surface area and the density of the hydrophobic tail region are interlinked properties. Hence, they should be examined in conjunction. The data are summarized in table 5. Our internal surface area per lipid for β-$C_8$Glc (41 Å$^2$) significantly exceeds the 38 Å$^2$ previously reported by Bogusz *et al.* [9]. Considering the lower concentration of water applied in their simulation and our range of values for different β-glycosides, we consider the values in reasonable agreement.

In thermotropic systems α-glycosides clearly shows both, higher surface areas and lower densities than β-anomers. However, a different picture results for the lyotropic systems. Whereas the densities for the hydrophobic region are almost not affected by the presence of water, the size of the interphase changes significantly. Moreover α-glycosides display an inverse behaviour to β-anomers. The latter swell due to absorption of water, whereas the first seem to shrink. For the water concentration applied in our simulations (15%) β-glycosides show higher surface areas than α-glycosides.

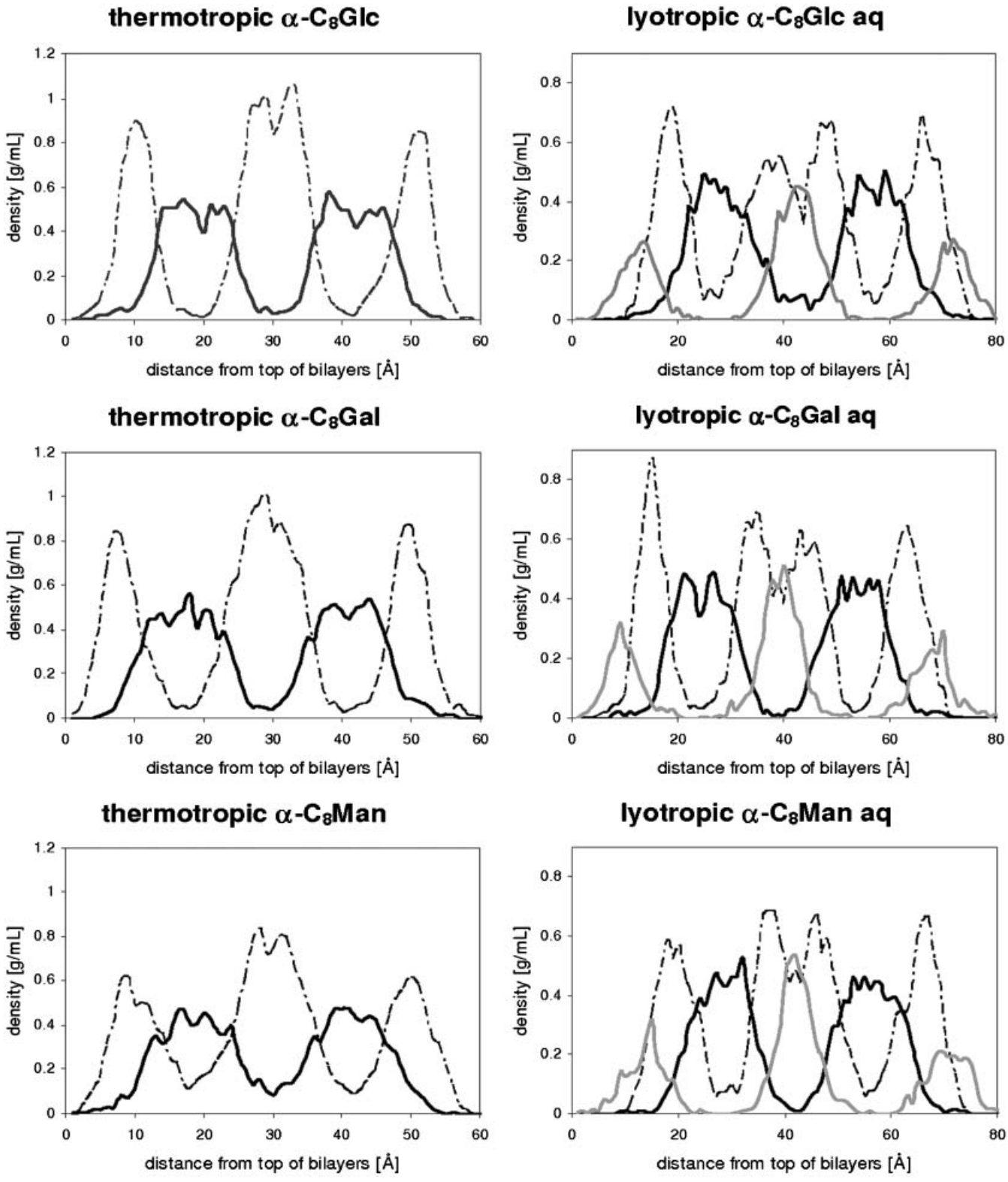


Figure 5. Local density profiles for α-glycosides (black=alkyl tail, broken=sugar head, grey=solvent=water).

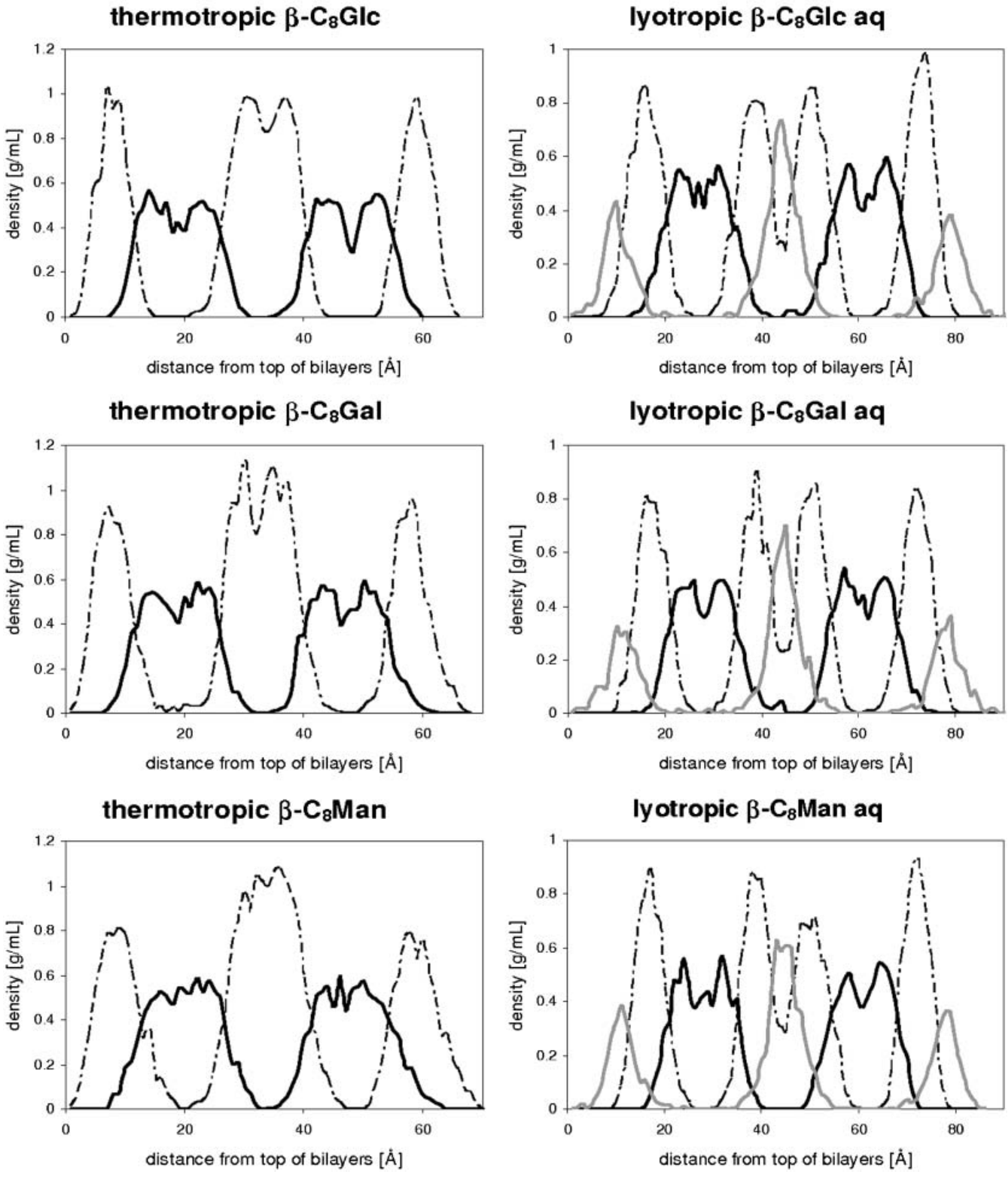


Figure 6. Local density profiles for $\beta$-glycosides (black=alkyl tail, broken=sugar head, grey=solvent=water).

Table 4. Bilayer spacing (COM=centre of mass; LDP=local density profile).

| | Thermotropic | | | Lyotropic | | |
|---|---|---|---|---|---|---|
| | COM | LDP | Ref. [5] | COM | LDP | Ref. [5] |
| α-Glc | 21.9±0.1 | 23±1 | 23.3 | 28.5±0.1 | 29±1 | – |
| α-Gal | 22.6±0.2 | 23±2 | – | 27.9±0.1 | 30±2 | – |
| α-Man | 20.9±0.3 | 23±2 | 23.1 | 27.4±0.1 | 29±1 | 24.3 (6% aq) |
| β-Glc | 28.9±0.1 | 29±1 | 25.6 | 34.62±0.01 | 35±1 | 29.7 (19% aq) |
| β-Gal | 28.1±0.1 | 28±1 | 25.8 | 33.2±0.2 | 34±1 | 28.2 (15% aq) |
| β-Man | 27.11±0.04 | 28±2 | – | 33.2±0.1 | 33±2 | – |

Table 5. Alkyl tail densities and internal microphase separation surfaces.

| | Thermotropic | | Lyotropic | |
|---|---|---|---|---|
| | Surface ($Å^2$/Lipid) | Density ($g\,ml^{-1}$) | Surface ($Å^2$/Lipid) | Density ($g\,ml^{-1}$) |
| α-Glc | 38.4±0.4 | 0.82±0.02 | 35.0±0.4 | 0.82±0.01 |
| α-Gal | 36.6±0.3 | 0.83±0.02 | 35.3±0.2 | 0.82±0.01 |
| α-Man | 38.1±0.2 | 0.83±0.02 | 36.0±0.4 | 0.82±0.01 |
| β-Glc | 35.8±0.3 | 0.95±0.01 | 41.4±1.5 | 0.95±0.02 |
| β-Gal | 35.8±0.3 | 0.95±0.01 | 40.3±1.0 | 0.93±0.01 |
| β-Man | 35.3±0.4 | 0.95±0.01 | 39.4±1.1 | 0.94±0.01 |



## 4. Discussion

### 4.1. *Validity of the total hydrogen bonding per lipid*

The maximum number of hydrogen bonding in this study is limited by the availability of suitable protons, unless we accept a proton to be involved in more than one hydrogen bonding. For the thermotropic system, the maximum total hydrogen bonding for one lipid is four, based on the four hydroxyl groups. There is also a more stringent constraint related to the availability of donor electron pairs. However, since the number of donors (six oxygen atoms) already exceeds the available protons, this limitation is irrelevant. The simulations determine the total intermolecular hydrogen bonding (excluding intramolecular hydrogen bonding) between 3.1 and 4.0 With our values for intramolecular hydrogen bonding of about 1.5 this adds up to total hydrogen bonding of nearly 5.5.

The difference of 1.5 is probably due to systematic errors during the hydrogen bonding standard calculation method based on the applied hydrogen bonding selection criteria. Applying the D–A distance instead of D–H–A, where A is the hydrogen acceptor and D is the hydrogen donor [16] (figure 2), increases the range for qualified hydrogen bonding. Also the selection tool does not limit the number of hydrogen bonding for a single hydrogen atom. If several qualified donor centres are found inside a hydrogen atom's qualifying range for hydrogen bonding, then all of them are counted instead of just the nearest or best positioned donor. Thus, our hydrogen bonding calculation is only qualitatively acceptable within the statistical range. This also applies for the lyotropic systems, although our result of 7.7 total hydrogen bonding per glycoside (involving both, inter- and intramolecular interactions) does not exceed the theoretical maximum. The latter is determined as 9.5 due to the availability of suitable hydrogen atoms (4 OH+2.75 water molecules, each worth 2, per glycoside). As stated before for the thermotropic systems, limitations based on acceptor availability do not apply.

### 4.2. *Validity of local density profiles*

LDPs were determined by single frame analyses only, owing to the extended calculation process. In order to avoid errors based on the modelling dynamics, we compared the LDPs for one frame at the beginning and one at the end of the simulation. Both LDPs showed no significant differences for any of the investigated systems. However, a more accurate approach requires a look on intermediate states as well. We therefore analysed the dynamics of the LDP for each one exemplary α- and β-glycoside, taking one frame out of every 1 ns production time (=1000 frames). The results, displayed in figure 7, indicate a steady state system without any significant change. The quasi-static behaviour is even more clearly visible by looking at the LDP derived bilayer spacings (table 6).

### 4.3. *Local densities*

The HyperChem® QSPR tool [14], used for the determination of regional densities, systematically

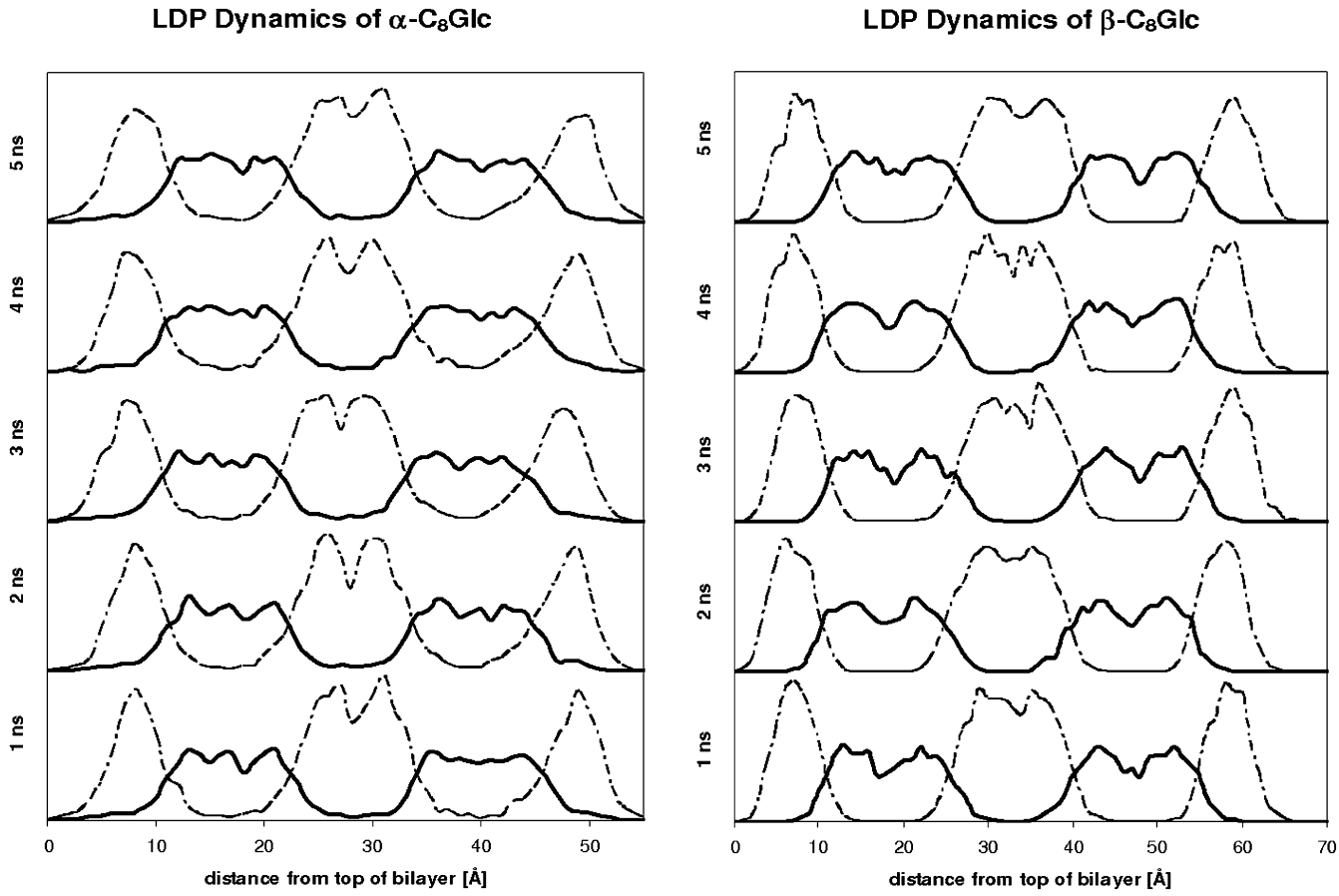


Figure 7. Local density profile dynamics (thermotropic systems) (black=alkyl tail, broken=sugar head).



Table 6. Dynamics of bilayer spacing based on LDP analysis.

| Frame | α-$C_8$Glc | β-$C_8$Glc |
|---|---|---|
| 1 ns | 22.5±1.3 | 29.0±1.4 |
| 2 ns | 22.8±1.3 | 28.8±1.5 |
| 3 ns | 22.5±1.3 | 29.0±1.4 |
| 4 ns | 23.0±1.0 | 28.5±1.3 |
| 5 ns | 22.8±1.3 | 29.0±1.4 |

overestimates the density of the hydrophobic region for the applied glycosides. This conclusion results from comparison of the determined values (table 5) with the experimental density for the corresponding hydrocarbon, i.e. octane (0.8 g ml$^{-1}$). Whereas α-glycosides basically seem to maintain the hydrocarbon's density, β-anomers exceeds this value by about 15%. It is unlikely, that such a drastic error is based on the simulation, especially since the corresponding values at the local density profiles, though systematically underestimated themselves, uniformly indicate drastically lower (>30%) densities everywhere inside the alkyl region. Therefore, we conclude, that the error must be due to the applied determination tool. However, a systematic error, while disqualifying for direct predictions, does not limit the use of the data for internal comparison.

### 4.4. α *and* β *anomers*

Sakya *et al.* [5] have explained differences in clearing points for glycoside anomers based on the internal microphase surface area as a result of the molecular shape of the surfactant. Amphiphilic liquid crystalline assemblies are supposedly driven by hydrogen bonding. Their thermal stability relies on the ability to store energy without disrupting the assembly. According to Sakya most energy will be stored in vibrations of the alkyl chains, due to low limitations based on intermolecular interaction for the hydrophobic region. Larger surface areas permit more vibrations and, therefore, reflect higher clearing points. An analogous explanation correlates lower tail group densities with increased liquid crystal stability. All experimental results so far have indicated higher clearing temperatures for pure α-glycosides than for the corresponding β-anomers. The thermotropic results displayed in

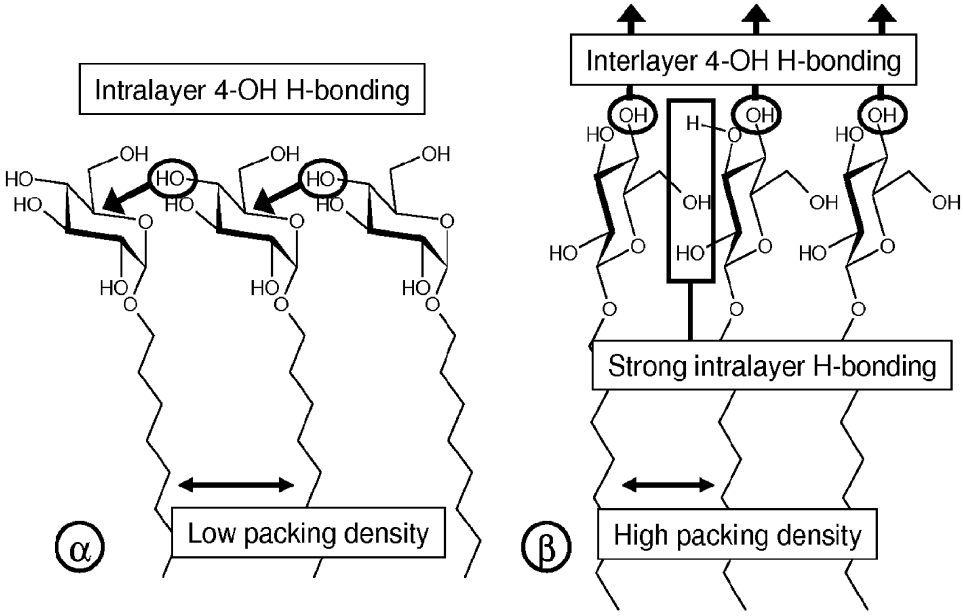


Figure 8. Packing density and hydrogen bonding for $\alpha/\beta$-anomeric pairs.



table 5 support these findings. An explanation is given in figure 8. The more linear shape of $\beta$-glycosides leads to a significantly more dense packing of the alkyl tails than for the bent shaped $\alpha$-anomers. However, neither the local tail region density nor the interface area can explain changes in transition temperatures within the $\alpha$- or $\beta$-anomeric groups. Thus the prediction ability for these tools is rather limited.

In lyotropic systems the hydrophobic density and the internal surface area lead to contradicting prediction for the clearing temperature of anomers. A significant effect of water on the surface area does not coincide with a change in the density of the alkyl region. In fact the latter is practically not affected. Since the local tail density is more directly related to vibrational freedom of the glycolipid, we consider this probe more suitable than the surface area. However, the limited availability of experimental data and varying concentrations prevent a proper checking of this prediction tool.

### 4.5. *Thermotropic systems*

As already stated before, $\alpha$-glycosides exhibit more hydrogen bonding than $\beta$-anomers (table 1). This corresponds to generally higher clearing temperatures for $\alpha$-compounds, which is in agreement with predictions based on the regional density for the alkyl tail (see above). However, the predictions in table 1 indicate an exception of this behaviour, either for galactose or for mannose, depending on the hydrogen bonding type (total or intralayer) applied in equation (1). With respect to identical total inter-glycoside hydrogen bonding for $\beta$-$C_8$Glc and $\beta$-$C_8$Gal we prefer to use intralayer hydrogen bonding for $\beta$-glycosides. This way, the predicted clearing point for the $\beta$-galactoside is higher than the one for the $\alpha$-anomer, thus contradicting Sakya's packing oriented theory [5] (see above). Only very few experimental data for clearing points of both galactosides are reported. However, the available data pairs indeed indicate a higher clearing temperature for the $\beta$-anomer [17, 18]. We would like to evaluate our intralayer hydrogen bonding based clearing points for $\beta$-glycosides by comparing predictions and experimental data for mannosides. The remarkably different predictions for the clearing point of $\beta$-$C_8$Man, based on either total inter-glycoside or intralayer hydrogen bonding, provides a good evaluation opportunity. Unfortunately, due to the difficult access of $\beta$-mannosides [19], no suitable experimental data are available.

The LDPs indicate local minima at the centres of the alkyl tail region for several glycosides. These minima are especially developed for $\beta$-anomers (figure 6) and are believed to originate from a systematic error in our layer arrangement. Due to our effort to minimize vacuum areas inside the simulation box, we arranged the tilted layers facing opposite directions (figure 9a). Unfortunately this arrangement limits the interception of alkyl tails from different layers, thus leading to a centre area of lower density. Another impact is a systematic overestimation of the bilayer spacing. The extent of the latter depends on the tilting

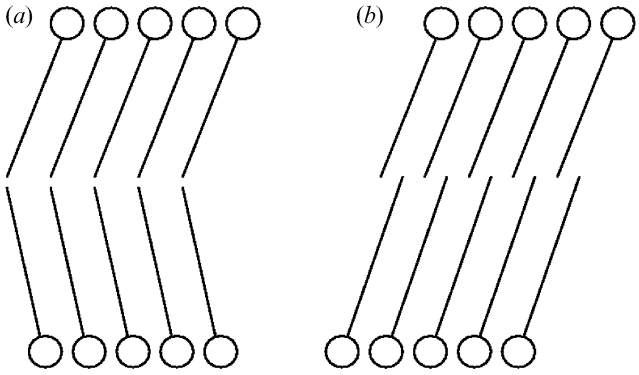


Figure 9. Arrangements of layers for modelling. (a) Tilted alkyl chains facing same direction, limited interdigitation; (b) antiparallel arrangement of alkyl chains, easy interdigitation of chains.

angle. β-Glycosides are significantly more tilted than α-anomers, therefore it is fitting that our bilayer spacing estimations for α-glycosides are more accurate than for the β-analogues. In order to evaluate the impact of the layer arrangement on our results, we repeated the simulation of β-$C_8$Glc using the more space requiring but easily interceptible parallel arrangement of the tilted tails (figure 9b). However, the simulation output for this arrangement, displayed in figure 10a, did neither significantly change the shape of the density profile (figure 10b) nor did it reduce the bilayer spacing or affect the hydrogen bonding results. Probably the required activation barrier for interlinking the alkyl tails of different layers is too high to be passed during the simulation. This means, that an improvement of bilayer predictions will require the full modelling of an interlinked bilayer. Interestingly we

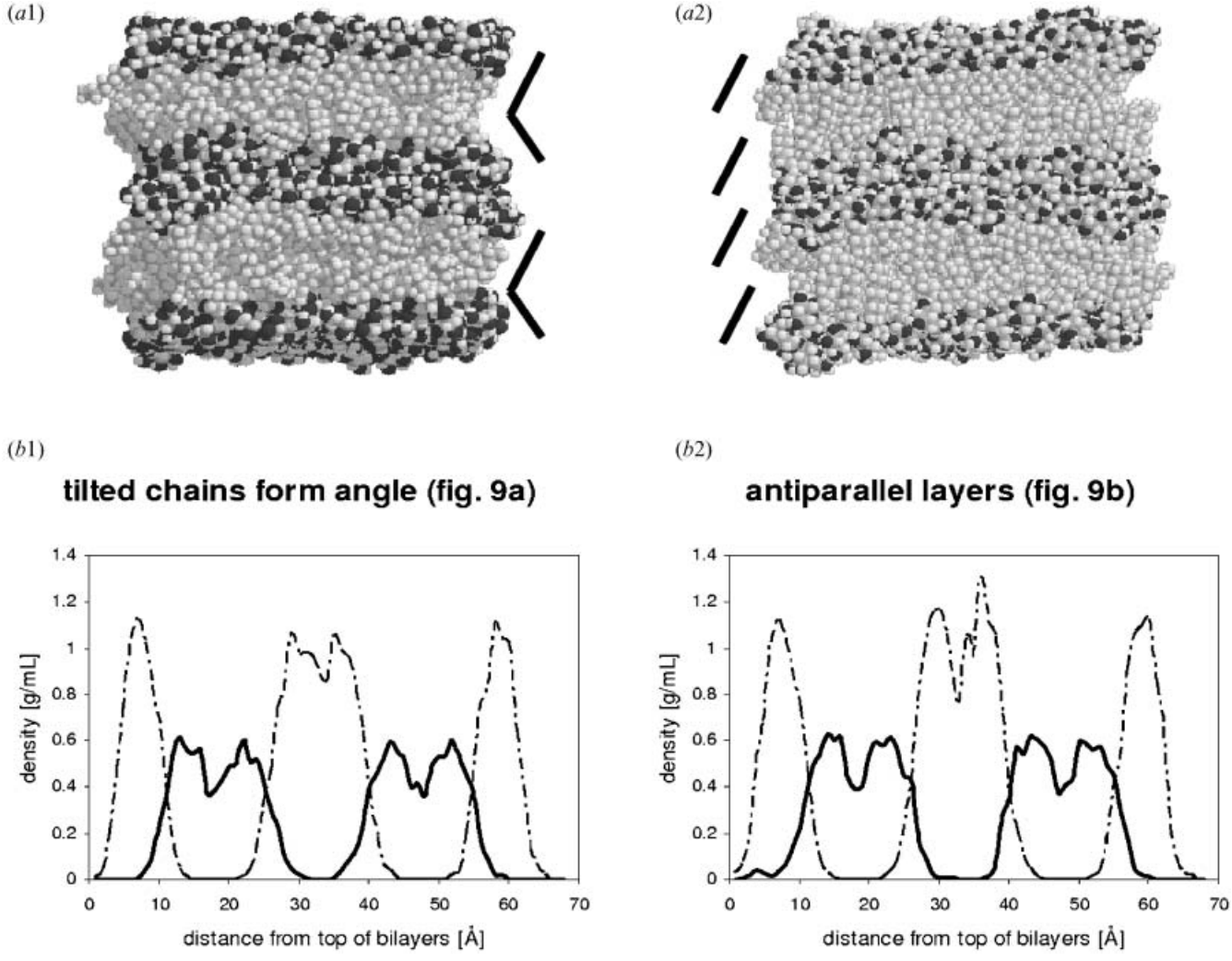


Figure 10. Impact of layer arrangement on simulation output. (a) Bilayer arrangement in overview, 1=tilted arrangement, 2=antiparallel arrangement; (b) local density profile.

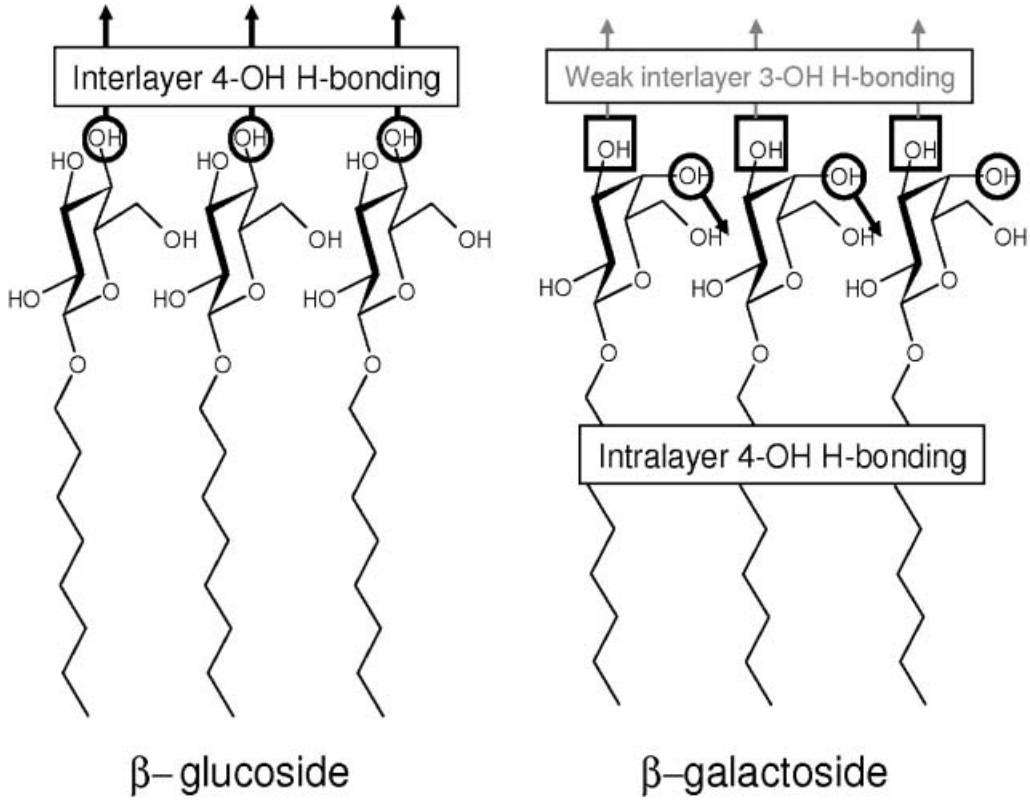


Figure 11. Stereochemical impact on the type of hydrogen bonding. The equatorial OH group in $\beta$-$C_8$Glc favours interlayer H bonding, whereas the axial OH group in $\beta$-$C_8$Gal leads to enhanced intralayer H bonding.



determined an analogous LDP minimum for the centre tail region of a previously reported dimyristoylglycerol phosphotidycholine (dmpc) lipid bilayer [20]. The local decrease of density (~25%) matches our findings. With respect to the different extent of minimum for $\alpha$- and $\beta$-glycosides, we still address this feature as an artefact. However, since our objective is rather focussing on the stability of bilayer assemblies than on their dimensions we consider such a measure beyond our scope. After all, the glycolipids' hydrogen bonding is unlikely to be affected by the extent of interdigitation of the alkyl tail region.

Differences for intra- and interlayer hydrogen bonding of anomeric ($\alpha/\beta$) as well as for epimeric pairs (e.g. Glc/Gal) can be explained based on the stereochemical arrangements. The linear arrangement of $\beta$-glycosides favours intralayer hydrogen bonding (figure 8), whereas the bent arrangement for $\alpha$-anomers enhance the opportunity for interlayer hydrogen bonding due to better accessibility of the hydroxyl groups. For $\beta$-Glc only the hydroxyl-group at C4 of the sugar really sticks out of the layer and provides reasonable access for interlayer hydrogen bonding. The $\alpha$-anomer, however, exposes the primary 6-OH, which due to the methylene spacer between the ring and the hydroxyl group is more flexible than secondary OHs. Thus it is not surprising, that $\alpha$-glycosides exhibit higher interlayer hydrogen bonding than $\beta$-anomers. Naturally we should expect a reverse trend for the intralayer hydrogen bonding. The data in table 1 show the expected trend. Nonetheless, the extraordinary low interlayer hydrogen bonding for the mannoside remains surprising.

Figure 11 shows the effect of the stereochemical orientation of a hydroxyl group on its hydrogen bonding preference. The equatorial 4-OH in $\beta$-$C_8$Glc gives rise for interlayer H-bonding, while its axial analogue in $\beta$-$C_8$Gal prefers intralayer interaction. With respect to this, we expect more intralayer and less interlayer hydrogen bonding for $\beta$-Gal than for $\beta$-Glc. Table 1 confirms this expectation. In fact the interlayer hydrogen bonding for $\beta$-Gal is likely to rely more on the 3-OH and the 6-OH groups. Figure 11 indicates the exposure of the $\beta$-$C_8$Gal 3-OH for interlayer hydrogen bonding. However, since C3 is embedded deeper inside the layer than C4, we should expect a lower contribution to interlayer hydrogen bonding compared to an axial 4-OH. For the corresponding $\alpha$-pair we expect the opposite behaviour. Based on the different hydrogen bonding preference of the 4-OH for anomers (figure 8) $\alpha$-Gal should expose higher interlayer and lower

intralayer hydrogen bonding for than α-Glc. Again table 1 confirms the expectation.

### 4.6. *Lyotropic systems*

The internal microseparation surface area, as well as the bilayer spacing, behaves oppositely for α- and β-glycosides (tables 4 and 5). Whereas water addition leads to an increase for β-anomers, α-anomers seem to contract. This behaviour is closely connected to differences in lyotropic LDPs, where β-glycosides show significantly higher separation of bilayer head groups than α-anomers. An explanation can be given as follows. β-Glycosides form compact layer structures. The possibility for water to penetrate the layers is low, thus water addition leads to a thin film separating the bilayers. This arrangement naturally drastically reduces interlayer hydrogen bonding between glycolipids, while intralayer hydrogen bonding is only slightly affected. Table 3 confirms this expectation. α-Glycoside based bilayers, on the other hand, are less compact. Because of this, water can be absorbed inside the layers, thus avoiding an expansion of the overall layer spacing. The impact of water on interlayer hydrogen bonding is expectedly lower than for β-anomers (table 3). Finally, the contraction of the bilayers may be explained based on an increase of the overall intralayer cohesion. This force is mediated both by intralayer glycoside interactions as well as by water mediated glycoside interactions. Increased intralayer cohesion can lead to a more staggered sugar packing, thus reducing both bilayer spacing and internal surface area. The slightly increased slope for the head group in lyotropic LDPs for α-glycosides (figure 5) is an indication of such a process.

The effect in hydrogen bonding upon water addition may also be applied for estimation of water solubilities. Since aqueous solutions of glycosides are based on micelles, intralayer hydrogen bonding is supposedly only minor affected. Comparing the intralayer hydrogen bonding of octyl β-glucoside and octyl β-galactoside bilayers (β-$C_8$Glc 2.4 $mol^{-1}$, β-$C_8$Gal 2.6 $mol^{-1}$) to those for the corresponding micelles (β-$C_8$Glc 0.9 $mol^{-1}$, β-$C_8$Gal 1.1 $mol^{-1}$) [21] we observe a decrease of about 60%. The lowering of hydrogen bonds is to be expected with respect to increased curvature. The constant ratio for hydrogen bonding of the two glycosides in micelle and in bilayer, however, indicates their close relationship. Interlayer hydrogen bonding, on the other side, is completely eliminated upon forming a solution. Therefore a drastic reduction of interlayer hydrogen bonding upon water treatment should refer to relatively good water solubility. Indeed, as predicted from table 3, the water solubility of β-$C_8$Glc is remarkably higher than the one for α-$C_8$Glc.

## 5. Conclusions

Computer simulations have proven useful tools for understanding layer-type assemblies of glycosides. Besides presenting images, they provide characteristic data, which can be correlated to experimentally observable physical properties. These correlations lead to an improved understanding of self-assembly and offer prediction tools for new materials. The literature proposed assumption of increased packing density for the lipophilic region in α-glycosides compared to those in β-anomers [5] could be confirmed. However, this density proved a fable prediction tool, since, despite differences in clearing points for stereoisomeric glycosides, neither the values for α- nor the ones for β-glycosides seem to depend on the configuration of the sugar. Varying clearing temperatures for stereoisomeric glycosides can be explained more generally based on differences for the intermolecular hydrogen bonding between glycosides. Quantitative correlations of this hydrogen bonding and the clearing temperature led to reasonable agreement with experimental data. For stereoisomers showing identical values for the total inter-glycoside hydrogen bonding, the intralayer hydrogen bonding can be applied instead, again leading to good agreement with experimental results. This suggests that a major criterion for the stability of layer-structured assemblies for glycosides is the extent of intralayer hydrogen bonding. However, with respect to missing experimental data for two out of six compounds in the investigated series, these conclusions certainly require further evaluation, e.g. by filling the gaps for clearing temperatures.

## Acknowledgements

We would like to thank the Ministry of Science, Technology and the Innovation (MOSTI) for the grants 09-02-0309010 SR0004/04 (Glycolipids Science & Technology) and 34-02-03-4001 (E-science GRID) sponsoring this research; Dr Richard Bryce, School of Pharmacy and Pharmaceutical Sciences, University of Manchester, UK and Prof. Vill, University of Hamburg, Germany, for inspiring discussions; the Faculty of Engineering, University of Malaya for providing access to their computer facilities, namely the UM Geranium CRAY Cluster and MIMOS Berhad, Technology Park Malysia for use to their AMD Opteron™ cluster.

## References

[1] *Anatrace Product Catalog 2002/2003* 6th Edn, pp. 78–79 (2003).
[2] W. Rybinnski, K. Hill. *Angew. Chem. Int. Ed.*, **37**, 1328 (1998).

[3] H. Kiwada, H. Niimura, Y. Fujisaki, S. Yamada, Y. Kato. *Chem. Pharm. Bull.*, **33**, 753 (1985).
[4] H. Kiwada, I. Nakajima, H. Matsuura, M. Tsuji, K. Yuriko. *Chem. Pharm. Bull.*, **36**, 1841 (1988).
[5] P. Sakya, J.M. Seddon, V. Vill. *Liq. Cryst.*, **23**, 409 (1997).
[6] V. Vill, R. Hashim. *Curr. Op. Colloid Interface Sci.*, **7**, 395 (2002).
[7] A.R. Van Buuren, H.J.C. Berendsen. *Langmuir*, **10**, 1703 (1994).
[8] S.E. Feller, R.M. Venable, R.W. Pastor. *Langmuir*, **13**, 6555 (1997).
[9] S. Bogusz, R.M. Venable, R.W. Pastor. *J. phys. Chem. B*, **104**, 5462 (2000).
[10] S. Ohta-lino, M. Pasenkiewicz-Gierula, Y. Takaoka, H. Miyagawa, K. Kitamura, K. Akhiro. *Biophys. J.*, **81**, 217 (2001).
[11] S. Abeyguanartne, R. Hashim, V. Vill. *Phys. Rev. E*, **73**, 011916 (2006).
[12] D.A. Case, D.A. Pearlman, J.W. Caldwell, T.E. Cheatham III, J. Wang, W.S. Ross, C. Simmerling, T. Darden, K.M. Merz, R.V. Stanton, A. Cheng, J.J. Vincent, M. Crowley, V. Tsui, H. Gohlke, R. Radmer, Y. Duan, J. Pitera, I. Massova, G.L. Seibel, U.C. Singh, P. Weiner, P.A. Kollman. *Amber7 Manual*, pp. 208 and 224, University of California (2002).
[13] H.A. Van Doren, L.M. Wingert. *Mol Cryst. liq. Cryst.*, **198**, 381 (1991).
[14] O. Ivanciuc. *J. Chem. Inf. Comput. Sci.*, **36**, 919 (1996).
[15] V. Vill, T. Böcker, J. Thiem, F. Fischer. *Liq. Cryst.*, **8**, 349 (1989).
[16] I.Y. Torshin, I.T. Weber, R.W. Harrison. *Protein Engng*, **15**, 359 (2002).
[17] V. Vill, H.M. von Minden, M.H.J. Koch, U. Seydel, K. Brandenburg. *Chem. Phys. Lipids*, **104**, 75 (2000).
[18] R. Hashim, H.H. Abdalla Hashim, N.Z. Mohd. Rodzi, R.S. Duali Hussen, T. Heidelberg. *Thin Solid Films*, **509**, 27 (2006).
[19] T. Tsuda, R. Arihara, S. Sato, M. Koshiba, S. Nakamura, S. Hashimoto. *Tetrahedron*, **61**, 10719 (2005).
[20] A.A. Gurtovenko, H. Tatra, M. Karttunen, I. Vattulainen. *Biophys. J.*, **86**, 3461, PDB file www.apmaths.uwo.ca/~mkarttu//downloads (dmpc128_20ns.pdb) (2004).
[21] T.C. Teoh, R. Hashim, R.A. Bryce. *J. phys. Chem. B*, **110**, 4978 (2006).